

Sawtooth curve of neutron multiplicity

U. Brosa

Fachbereich Physik, Philipps-Universität, D-3550 Marburg, West Germany
 (Received 28 March 1985; revised manuscript received 1 July 1985)

Results of detailed calculations which reproduce the sawtooth dependence of neutron multiplicity on fragment mass in nuclear fission are presented. The same sawtooth seems to occur in deep-inelastic heavy-ion reactions when target and projectile are sufficiently unequal. These results support an idea by Whetstone and suggest a way to include shell effects which is different from that employed in the scission-point models.

The most successful model of nuclear fission presently is that by Wilkins, Steinberg, and Chasman.¹ It describes several striking trends in the fission of the actinides in at least semiquantitative agreement with data. There is, however, a principal objection against the model: It assumes metastability at the scission point in contradiction to the foundations of fission theory, viz., that the gross properties of fission can be understood by the changing preponderance of surface against Coulomb energy. In fact, the scission point is a particularly unstable configuration, and this remains true if shell effects are included.² Such a principal objection is nevertheless useless unless measurable properties prove the insufficiency. One such property is the prodigious width of the mass distributions created by fission. This was already discussed in Ref. 3, and the experimental facts are well settled. Another property to be discussed in this note is the occurrence of the sawtooth curve of the multiplicity of evaporated neutrons at high excitation energies. The sawtooth in low-energy fission was explained by Brunner and Paul,⁴ and by Vandenbosch⁵ as being due to shell effects in the nascent fragments. In particular, Vandenbosch's paper is a very transparent exposition of the underlying idea, and exactly this idea is exploited in the scission-point model by Wilkins *et al.* However, since shell effects quickly die out with rising nuclear temperature,⁶ the scission-point model should deny the existence of the sawtooth at high excitation energies.

Data will be shown which demonstrate a remarkable persistence of the sawtooth with increasing excitation. There even seems to be an indication for its occurrence in deep-inelastic heavy-ion reactions with excitation energies of more than 100 MeV. The last point, however, needs further examination, and an experiment was proposed giving a detailed prediction of its outcome.⁷

An explanation in remarkable contrast to the model by Wilkins *et al.* was given by Whetstone many years before.⁸ We have now developed his idea to the extent that it yields quantitative predictions. Furthermore, we have established that the trigger which puts Whetstone's mechanism into action is actually the same instability which challenges the scission-point model. Our implementation of Whetstone's mechanism is published elsewhere,⁹ together with numerous applications to symmetric fission³ and heavy-ion reactions.^{7,9} Here some applications to asymmetric fission will be reported, which were obtained, as should be stressed, without a single modification of the basic algorithms used for previous work. But even without knowing the computational details, the mechanism can be understood by considering Fig. 1.

The heavy line in the central part of Fig. 1 shows the nuclear shape just before scission, and this very shape is, according to Whetstone's approach, the origin for most phenomena in fission. The mass distribution results from the fluctuations of that position where the neck starts to stragulate; the maximum of the mass distribution is caused by decays which occur close to the position of smallest neck

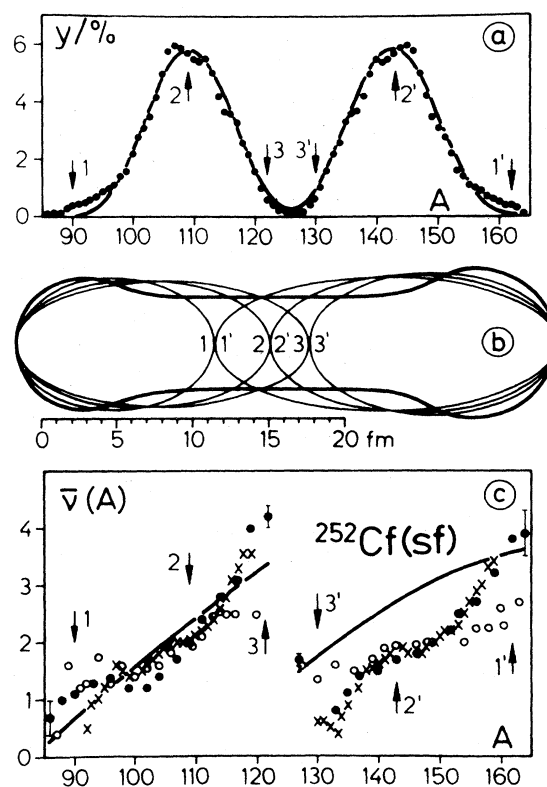


FIG. 1. Mass yield Y and neutron multiplicity $\bar{\nu}(A)$ as functions of the fragment's mass number A for the spontaneous fission of ^{252}Cf . The dots in (a) represent data taken from Ref. 12; those in (c) stem from Bowman *et al.* (Ref. 20). Stars refer to results by Terrell (Ref. 21), and open circles to measurements by Whetstone (Ref. 8). Drawn lines are calculated using our model (Refs. 3 and 9). (c) is so far superior to Fig. 9 in Ref. 1, as here the computed and measured neutron multiplicities are compared directly, whereas there computed deformations are related to measured multiplicities.

diameter, and the width of the mass yield reproduces the amount of mass contained in the neck. Therefore, one might consider the mass yield, shown in Fig. 1(a), as a faithful picture of the nucleus just before scission, were it not for the following ambiguity: A very long shape with a very thin neck would deliver the same mass distribution as a short shape with a thick neck. This ambiguity was resolved by our work. Following a hint by Griffin and Kan,¹⁰ we obtained a universal relation between the shape's length l and its neck radius r_n : $l = 11r_n$ [Eq. (15e) in Ref. 9]. Using this relation, one finally establishes a one-to-one mapping between mass yields and prescission shapes. The drawn line in Fig. 1(a) shows the calculated mass distribution which ensues from fixing the position of smallest neck diameter and the total length of the shape [Fig. 1(b)] by maximum and width of the experimental mass distribution.

The decay at various positions of the neck yields various deformations of the nascent fragments which are approximated, for computational simplicity, by spheroids. This again gives rise to strongly varying excitation energies of the fully accelerated fragments, and the excitation energy finally is converted into evaporation of neutrons. Therefore, it is a simple matter to compute from the available energy of the nascent fragments,

$$E^*(A) = E_{\text{def}}(A) + E_s^* A / A_{\text{cn}}, \quad (1)$$

the neutron multiplicities as shown in Fig. 1(c). Here A_{cn} denotes the mass number of the compound nucleus, A that of the fragment, E_{def} its deformation energy just after scission [see Fig. 1(b)], and the last term in Eq. (1) is the share in thermal energy E_s^* of the shape just after scission which the fragment gets, according to equipartition. All numbers on the right-hand side of Eq. (1) are easily calculated when the shape is known, i.e., when the experimental mass distribution is known, and when the total excitation energy is given.

In Fig. 1(b) a few partitions into fragments are displayed, and the corresponding points in the data are indicated by the numbers. One has only to remember that the neutron multiplicity is a monotonic function of the fragment's deformation in order to conclude that an asymmetric mass yield must always be accompanied by a sawtoothlike multiplicity function.

The spheroids in Fig. 1(b) are charged, and thus they repel each other. When the fragments accelerate, the potential energy of repulsion at scission converts into the total kinetic energy E_k of the completely separated nuclei, provided the prescission kinetic energy is small (≤ 10 MeV). This, however, can be inferred from experiments with long-range alpha particles.¹¹ Hence, the total kinetic energy is closely related to the length of the prescission shape. The average total kinetic energy \bar{E}_k calculated from the prescission shape in Fig. 1(b) is 186 MeV—in perfect agreement with experiment.¹²

When some experimental information is given, our model permits the computation of additional measurable quantities. Our standard strategy is as follows:

(a) From the known mass yield, i.e., its centroid \bar{A} and width σ_A , and from the excitation energy E^* of the compound nucleus, we compute the average total neutron multiplicity $\bar{\nu}_{\text{tot}}$, the individual multiplicities $\bar{\nu}(A)$ for every fragment, and the average total kinetic energy \bar{E}_k .

However, in most cases the data is by far not as complete

as it is for the spontaneous fission of ²⁵²Cf. The mass yield, for example, or the excitation energy may be badly determined. Therefore, we have adopted two additional methods:

(b) If \bar{A} , E^* , and \bar{E}_k are known, σ_A , $\bar{\nu}_{\text{tot}}$ and $\bar{\nu}(A)$ can be found.

(c) If \bar{A} , σ_A , and $\bar{\nu}_{\text{tot}}$ are given, E^* , $\bar{\nu}(A)$, and \bar{E}_k are the results of our theory.

Methods (b) and (c) just require the solving of the same equations as in (a) for other variables. It will be noted that the most detailed piece of information $\bar{\nu}(A)$ appears always as output.

The two terms in Eq. (1) may have very different weights at different excitation energies. For example, for low-energy fission the second term is small, but for deep-inelastic heavy-ion reactions it is by far the dominant one. Still, the first term is there and causes a jump at the symmetric partition. These differences are illustrated by Figs. 2, 3, and 4.

In Fig. 2 the neutron multiplicities of fission events with very high E_k are collected. Larger E_k means less excitation energy E_s^* , i.e., the second term in Eq. (1) yields contributions so small that they are not sufficient to evaporate a single neutron. The sawtooth, however, is present, which indicates that Fig. 2 is a pure result of deformational variation—the effect depicted by Fig. 1(b). Here our model gives $l = 31.0$ fm as the total length of the shape, whereas it was $l = 35.4$ fm for the case shown in Fig. 1.

Figure 3 reproduces results from the fission of ²³⁸U at two different excitation energies. The structure of this data is similar to that for ²⁵²Cf in Figs. 1 and 2: Higher excitation energy just lifts the sawtooth upwards without destroying it. This is in marked contrast to the expectations from the scission-point model.

The surprising persistence of the sawtooth seems to occur also in deep-inelastic heavy-ion reactions. Figure 4 shows neutron multiplicities for events with large energy loss ($84 \text{ MeV} < E_{\text{loss}} < 236 \text{ MeV}$). The discontinuity at symmetry shown in Fig. 4 was interpreted by the authors of Ref. 13 as being caused by the emission of charged particles, in particular, of alphas. These particles, however, were not measured. More recent investigations indicate that the alpha multiplicities per fragment are too small: 0.3 in fission¹⁴

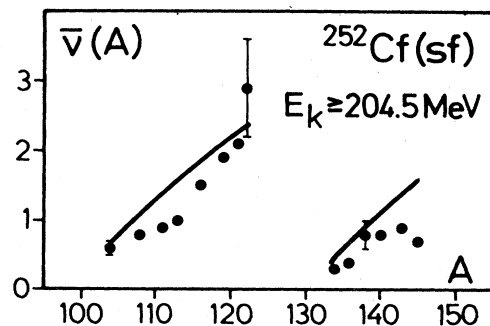


FIG. 2. Neutron multiplicity $\bar{\nu}(A)$ as a function of the mass number A for the spontaneous fission of ²⁵²Cf, where only events with total kinetic energy of about 204.5 MeV were admitted. Data are from Ref. 20; the line displays our theoretical results. Here, as in Fig. 1, only some typical error bars given by the experimentalists are shown.

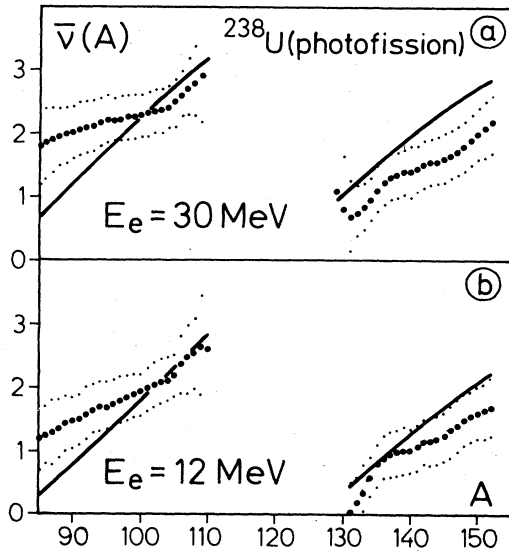


FIG. 3. Neutron multiplicity $\bar{\nu}(A)$ over mass number A for the photofission of ^{238}U . Data were read from Fig. 4 in Ref. 22. Heavy dots denote the averages; light points mark the range of experimental errors. E_e is the energy of the electrons which produce the bremsstrahlung. The drawn lines are from our model.

and 0.2 in deep-inelastic collisions,¹⁵ whereas it should be not less than 0.5 if the explanation by evaporation were correct. Therefore, an alternative or additional explanation might be useful. It seems impossible to attribute the discontinuity at such high excitation energies to shell effects. For Whetstone's mechanism, however, this jump is a necessary consequence from an asymmetric precission shape. Indeed, the shape which results in the exit channel of a deep-inelastic collision between two sufficiently different nuclei is similar to that in Fig. 1(b),^{7,9} but it takes no

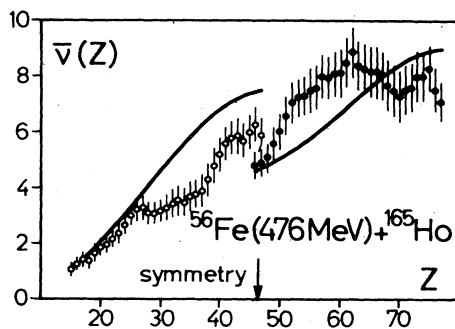


FIG. 4. Neutron multiplicity $\bar{\nu}(Z)$ as a function of the fragment's charge number Z for the deep-inelastic heavy-ion reaction Fe on Ho. The paper of Hilscher *et al.* (Ref. 13) is the source of the data, and the lines exhibit the theoretical outcome. In heavy-ion reactions, the neutrons can be identified as coming from the projectilelike fragments (open symbols) or from the targetlike ones (closed symbols). This yields, for the charge numbers close to symmetry, a two-valued function, and it is interesting to note that Whetstone's mechanism actually demands the occurrence of two branches, since, for an asymmetric precission shape, every nucleus with fixed A and Z can be produced with two different deformations. Consult Fig. 1(b) for the visualization of this fact.

shell contributions whatsoever to produce it. Instead, inertia and minimization of surface energy seem to cause its asymmetry.⁷

A few technical remarks should be made on how exactly the calculations for Figs. 1–4 were performed. Figure 1 results from a straightforward application of method (a). Figure 2 was produced by method (b), where it was assumed that \bar{A} is the same as in Fig. 1 and $\bar{E}_k = 204.5$ MeV. For both Figs. 1 and 2 E^* was estimated to be of the order of the fission barrier, and the sensitivity with respect to this parameter was checked. Figures 3 and 4 were obtained by method (c). For Fig. 3, \bar{A} and σ_A^2 were taken from a systematics.¹⁶ For Fig. 4 average charge number \bar{Z} and charge variance σ_Z^2 were assumed to be 26 and 40, respectively, and these numbers were converted to \bar{A} and σ_A^2 using the simplest scaling.

Finally, four problems have to be discussed. The first is on the dependence of shell effects on nuclear temperature. From the data shown in Fig. 3, it seems difficult to attribute the sawtooth to the shell structure in the fragments. An excitation energy $E^* = 16$ MeV in ^{238}U as in Fig. 3(a) would lead to a reduction of shell contributions by a factor of 2.⁶ In this estimate it is assumed that the nucleus gains about 14 MeV when the neck snaps, i.e., $E_s^* \approx 30$ MeV, as can be found from a careful analysis of energy conservation. The data in Fig. 3(a), however, shows no diminution of the sawtooth. Whetstone's mechanism gets along without shells in the fragments, but it is based on the assumption of an asymmetric precission shape. There is presently not the slightest hope to explain, in nuclear fission, such a shape without shell effects. Why should the shells in the nascent fragments vanish while they survive in the fissioning nucleus? A possible answer is that the fragments are hotter than the precission nucleus, since the snapping converts potential energy into excitation exactly at scission. The numbers given above indicate that this is not a small effect. If this answer were correct, one should expect the disappearance of the sawtooth at an excitation energy E^* of more than 30 MeV (snapping not included).

Thus, in nuclear fission questions on the disappearance of shell effects and on the mechanism at scission will be always intermingled. This is different with deep-inelastic heavy-ion reactions. The asymmetric precission shape is just a consequence of the asymmetric entrance channel configuration, and it is possible to examine the dependence of the effect on excitation energy by varying the impact energy.

The second problem is to understand the undeniable usefulness of the scission-point model. Here numerical work^{2,17,18} may be helpful. It suggests the formation of shell structures in the fissioning nucleus similar to those in the nascent fragments long before scission takes place. Therefore, it is likely that, on the average, the dynamics of fission drive the system to a configuration close to that which one would obtain by considering just the statics at the scission point.

The third problem concerns a serious deficiency of Whetstone's mechanism: Without an essential modification it cannot explain the dip in the distribution of total kinetic energy as a function of fragment mass, e.g., for uranium.⁵ This remains true also for our implementation, the culprit being the above mentioned relation $l = 11r_n$. The relation is, as we have shown in previous publications (see Ref. 7 and the references therein), a result only of surface tension and inertia. Coulomb repulsion and angular momentum are

unimportant, since they only add slowly with l varying contributions to the potential energy of the fissioning nucleus. This is different with shell contributions. The pictures presented by Pashkevich¹⁸ for uranium suggest that the shell contributions suppress the formation of symmetric pre-scission shapes, but, if by a fluctuation such a shape emerges, it should be extraordinarily stable against scission. In this case the above relation should read $l = 14r_n$, where the number 14 must be considered as a preliminary result, since we are working on this modification. The unusually long shape would lead to reduced Coulomb repulsion, and the dip in the kinetic energy would become understandable.

The fourth problem is to clarify a difference to previous work on nuclear fission.^{2,19} The claim that a thorough

understanding of the dynamics from saddle to scission is necessary for a complete explanation of the data is not new, but is only supported by this work. The reason why only partial success was allotted to such dynamic models seems to be in their too restricted number of degrees of freedom. As a consequence, important instabilities are suppressed. In particular, this is true for the radius of the neck and its curvature, which are not independent degrees of freedom in former models of nuclei fission.

I am grateful to S. Grossmann for many discussions and his careful reading of this paper. R. Brandt and W. Westmeier made some very stimulating suggestions, and D. Hilscher supported this work by several arguments.

-
- ¹B. D. Wilkins, E. P. Steinberg, and R. R. Chasman, *Phys. Rev. C* **14**, 1832 (1976).
- ²P. Möller and J. R. Nix, in *Proceedings of the Third International Atomic Energy Agency Symposium on Physics and Chemistry of Fission, Rochester, 1973* (IAEA, Vienna, 1974), Vol. I, p. 103, in particular Fig. 6.
- ³U. Brosa and S. Grossmann, *Z. Phys. A* **310**, 177 (1983).
- ⁴W. Brunner and H. Paul, *Ann. Phys. (Leipzig)* **8**, 146 (1961), where former work is also quoted.
- ⁵R. Vandenbosch, *Nucl. Phys.* **46**, 129 (1963).
- ⁶A. Bohr and B. R. Mottelson, *Nuclear Structure* (Benjamin, New York, 1975), Vol. II, p.607. The relevant thermodynamic quantity for fission is the free energy, as discussed on p. 371.
- ⁷S. Grossmann and U. Brosa, *Z. Phys. A* **319**, 327 (1984).
- ⁸S. L. Whetstone, *Phys. Rev.* **114**, 581 (1959).
- ⁹U. Brosa and S. Grossmann, *J. Phys. G* **10**, 933 (1984).
- ¹⁰J. J. Griffin and K.-K. Kan, *Rev. Mod. Phys.* **48**, 467 (1976).
- ¹¹C. R. Guet, H. A. Nifenecker, C. Signarbieux, and M. Ashgar, in *Proceedings of the Fourth International Atomic-Energy Agency Symposium on Physics and Chemistry of Fission, Jülich, 1979* (IAEA, Vienna, 1979), Vol. II, p. 247.
- ¹²J. P. Unik, J. E. Gindler, L. E. Glendenin, K. F. Flynn, A. Gorski, and R. K. Sjoblom, in *Proceedings of the Third International Atomic-Energy Agency Symposium on Physics and Chemistry of Fission, Rochester, 1973* (IAEA, Vienna, 1974), Vol. II, p. 19.
- ¹³D. Hilscher, J. R. Birkelund, A. D. Hoover, W. U. Schröder, W. W. Wilcke, J. R. Huizenga, A. C. Mignerey, K. L. Wolf, H. F. Breuer, and V. E. Viola, Jr., *Phys. Rev. C* **20**, 576 (1979).
- ¹⁴W. W. Wilcke, J. P. Kosky, J. R. Birkelund, M. A. Butler, A. D. Dougan, J. R. Huizenga, W. U. Schröder, H. J. Wollersheim, and D. Hilscher, *Phys. Rev. Lett.* **51**, 99 (1983).
- ¹⁵J. P. Kosky, W. W. Wilcke, J. R. Birkelund, M. A. Butler, A. D. Dougan, J. R. Huizenga, W. U. Schröder, H. J. Wollersheim, and D. Hilscher, *Phys. Lett.* **133B**, 153 (1983).
- ¹⁶K. F. Flynn, E. P. Horwitz, C. A. A. Bloomquist, R. F. Barnes, R. K. Sjoblom, P. R. Fields, and L. E. Glendenin, *Phys. Rev. C* **5**, 1725 (1972).
- ¹⁷D. Scharnweber, W. Greiner, and U. Mosel, *Nucl. Phys.* **A164**, 257 (1971).
- ¹⁸V. V. Pashkevich, *Nucl. Phys.* **A169**, 275 (1971).
- ¹⁹J. R. Nix and W. J. Swiatecki, *Nucl. Phys.* **71**, 1 (1965).
- ²⁰H. R. Bowman, J. D. Milton, S. G. Thompson, and W. J. Swiatecki, *Phys. Rev.* **129**, 213 (1963).
- ²¹J. Terrell, *Phys. Rev.* **127**, 880 (1962).
- ²²D. De Frenne, H. Thierens, B. Proot, E. Jacobs, P. De Gelder, A. De Clercq, and W. Westmeier, *Phys. Rev. C* **26**, 1356 (1982).